Original Article

A novel m6A/m5C/m1A/m7G-related classification and risk signature predicts prognosis and reveals immunotherapy inclination in gastric cancer

Ruyue Chen[1,2], **Lixin Jiang**[1,3]

[1]Medical College, Qingdao University, Qingdao, China; [2]Department of Gastrointestinal Surgery, Yantai Yuhuangding Hospital, Qingdao University, Yantai, China; [3]Department of General Surgery, Yantai Yeda Hospital, Yantai, China

Contributions: (I) Conception and design: R Chen; (II) Administrative support: L Jiang; (III) Provision of study materials or patients: R Chen; (IV) Collection and assembly of data: R Chen; (V) Data analysis and interpretation: R Chen; (VI) Manuscript writing: Both authors; (VII) Final approval of manuscript: Both authors.

Correspondence to: Lixin Jiang, MD. Medical College, Qingdao University, Ningxia Road 308, Qingdao 266071, China; Department of General Surgery, Yantai Yeda Hospital, No. 23-1 Huanghe Road, Yantai Economic and Technological Development Zone, Yantai 264006, China. Email: jianglixin_1969@163.com.

Background: Gastric cancer (GC) is characterized by high morbidity and mortality rates, and the prognosis is not optimistic. Therefore, the search for new biomarkers is crucial. Methylation modifications in RNA modifications play a crucial role in tumors. However, the role of methylation modification of integrated m6A/m5C/m1A/m7G, in GC and its related analysis have not been reported. It still needs to be studied in depth. Our study aims to deepen our understanding of m6A/m5C/m1A/m7G methylation and potentially provide new strategies for GC treatment.

Methods: We used TCGA-STAD (The Cancer Genome Atlas-Stomach Adenocarcinoma) as a training set and GSE84433 as a validation set to analyze and determine potential associations between m6A/m5C/m1A/m7G-related genes and clinical risk of GC. In addition, we explored the prognostic value and potential biological mechanisms of m6A/m5C/m1A/m7G-related genes in GC through consistent clustering, differential expression gene identification, enrichment analysis, and immune infiltration analysis. Finally, we constructed m6A/m5C/m1A/m7G-related risk signature (MRRS) to evaluate the correlation between risk grade and survival prognosis, drug sensitivity, and immune infiltration, and validated the validity by immunohistochemical staining.

Results: We identified subgroups of C1, C2, and C3 patients by consensus clustering using data from 45 m6A/m5C/m1A/m7G-related genes. The three groups showed significant differences in survival, immune scores, and immune cell infiltration. We then constructed MRRS using least absolute shrinkage and selection operator (LASSO) regression analysis, including *SLC5A6*, *FKBP10*, *GPC3*, and *GGH*, which could accurately differentiate between high-/low-risk populations. Its accuracy was further validated in the validation set and immunohistochemical staining. These results suggest that m6A/m5C/m1A/m7G are closely related to the GC tumor immune microenvironment, and MRRS has good performance in predicting the survival of GC patients.

Conclusions: In this study, we highlighted the association of m6A/m5C/m1A/m7G subtypes with changes in the GC immunotumor microenvironment. We constructed and validated MRRS, which is valuable in predicting survival, immune infiltration and drug sensitivity in GC patients. This helps to deepen our understanding of m6A/m5C/m1A/m7G methylation and potentially provides new strategies for GC treatment.

Keywords: Gastric cancer (GC); m6A/m5C/m1A/m7G; classification; immunotherapy; prognosis

Submitted Dec 19, 2023. Accepted for publication Jun 10, 2024. Published online Jul 26, 2024.
doi: 10.21037/tcr-23-2325
View this article at: https://dx.doi.org/10.21037/tcr-23-2325

Introduction

Gastric cancer (GC) is a health-threatening malignant tumor, which is one of the top five common cancers in the world with a high mortality rate (1-3). Early clinical symptoms in patients with GC have low specificity and are usually without significant discomfort. This leads to the unfortunate fact that GC patients are already in the advanced stages when they are first diagnosed, and the prognosis is not optimistic. Currently, the treatment of GC is still mainly based on surgery, and postoperative combined radiotherapy and chemotherapy and other comprehensive treatment (4-6). Despite the development of medical technology and the increase of diagnostic and therapeutic means for GC in recent years, the mortality rate of GC patients is still not encouraging (7-9). Therefore, it is particularly important to develop effective biomarkers and prognostic models as new therapeutic tools to improve the prognosis of patients (10-13).

Methylation is the most abundant method of RNA modification in eukaryotic mRNAs (14-16), and it is involved in a variety of physiological and pathological processes in body (17-19). Common methylation sites include n6-methyladenosine (m6A), 5-methylcytosine (m5C), n1-methyladenosine (m1A) and 7-methylguanosine (m7G) methylation sites (20-24). They modify target RNAs by binding to writers, erasers and readers (25,26). More importantly, a growing number of studies have shown that methylation also plays an important role in a wide range of cancers, with its involvement in cancers including breast, bladder, thyroid, colorectal, and esophageal cancers (27-32).

Although prognostic features associated with RNA methylation have now been established in some cancers (33-36), they often involve only a single RNA modification. Recent study on GC and methylation have shown the predictive role of three types of methylation (m6A, m5C and m1A) in GC (37). No studies have reported the relationship between GC and genes associated with the four major RNA methylation modifications, which still needs to be thoroughly investigated.

In this study, we synthesized various RNA modifications, developed and validated a novel m6A/m5C/m1A/m7G-related risk signature (MRRS), analyzed the prognostic value of MRRS in GC and differentiated patients with different levels of immunotherapeutic sensitivity. The aim was to demonstrate the value of MRRS in assessing the immune microenvironment and survival prognosis of GC patients, and to lay the foundation for the discovery of new potential therapeutic targets, paving the way for improved individualized patient treatment. We present this article in accordance with the TRIPOD reporting checklist (available at https://tcr.amegroups.com/article/view/10.21037/tcr-23-2325/rc).

Highlight box

Key findings

- m6A/m5C/m1A/m7G methylation are closely related to the gastric cancer (GC) tumor immune microenvironment, and m6A/m5C/m1A/m7G-related risk signature (MRRS) has good performance in predicting the survival of GC patients.

What is known and what is new?

- GC is characterized by high morbidity and mortality rates, and the prognosis is not optimistic. Methylation modifications in RNA modifications play a crucial role in tumors.
- We found the association of m6A/m5C/m1A/m7G methylation subtypes with changes in the GC immunotumor microenvironment. We constructed and validated MRRS, which is valuable in predicting survival, immune infiltration and drug sensitivity in GC patients.

What is the implication, and what should change now?

- Our study helps to deepen our understanding of m6A/m5C/m1A/m7G methylation and potentially provides new strategies for GC treatment.

Methods

Ethical statement

The study was conducted in accordance with the Declaration of Helsinki (as revised in 2013).

Data sources

For the training set, transcriptome information for a total of 407 TCGA-STAD (The Cancer Genome Atlas-Stomach Adenocarcinoma) cases, including 375 STAD samples and 32 normal samples, was downloaded from TCGA database (https://portal.gdc.cancer.gov/). Mutations and matched clinicopathologic data for the TCGA-STAD dataset were also obtained from the TCGA database. For the validation set, microarray gene chips from the Gene Expression Omnibus database (GEO, www.ncbi.nlm.nih.gov/geo/, GEO accession: GSE84433, Platforms: GPL6947), which contains 357 patients, were used.

Consensus clustering analysis of m6A/m5C/m1A/m7G-related subtypes

We identified 22 m6A-regulated genes, 13 m5C-regulated genes, 8 m1A-regulated genes, and 2 m7G genes from previous studies. M6A regulatory genes included *METTL3*, *METTL14*, *METTL16*, *WTAP*, *RBM15*, *RBM15B*, *ZC3H13*, *YTHDC1*, *YTHDC2*, *YTHDF1*, *YTHDF2*, *YTHDF3*, *IGF2BP1*, *IGF2BP2*, *IGF2BP3*, *HNRNPA2B1*, *HNRNPC*, *RBMX*, *FMR1*, *LRPPRC*, *ALKBH5*, and *FTO*. M5C regulated genes included *TRDMT1*, *NSUN2*, *NSUN3*, *NSUN4*, *NSUN5*, *NSUN6*, *NSUN7*, *DNMT1*, *DNMT3A*, *DNMT3B*, *ALYREF*, *YBX1*, and *TET2*. M1A regulated genes included *TRMT6*, *TRMT61A*, *TRMT61B*, *TRMT10C*, *BMT2*, *RRP8*, *ALKBH1*, and *ALKBH3*. M7G genes included *METTL1* and *WDR4*.

Cluster analysis was performed using ConsensusClusterPlus using aggregated km clusters with 1-log correlation distance and resampling 80% of the samples 10 times. The optimal number of clusters was determined using the area under the curve of the consistent cumulative distribution function, the K-value, and the within-group consistency to ensure stability of the results.

Identification and analysis of differentially expressed genes (DEGs)

Limma is a differential expression screening method that relies on generalised linear models. In this study, we utilized the R package limma (version 3.40.6) to perform differential analysis and identify the DEGs between the two groups. The screening criteria for DEGs were determined as the adjusted $P<0.05$ and $|\text{fold change}| >1.5$. Then, Gene Ontology (GO) and Kyoto Encyclopedia of Genes and Genomes (KEGG) analyses were carried out to compare the differential signal pathway and biological effects among the different Disulfidptosis-Related cluster cohorts. GO and KEGG enrichment analyses were premised on the q-value and P value thresholds of <0.05.

Mutation landscape analysis

We collected somatic mutation data from TCGA for patients with STAD in order to investigate genetic structural changes between different groups and to create waterfall plots to visualize mutated genes.

Construction and validation of the MRRS

Least absolute shrinkage and selection operator (LASSO) is a common regression analysis method that combines variable selection and regularization to enhance the predictive performance and interpretability of the resulting statistical model. In this study, we employed the R package glmnet to conduct regression analysis using the LASSO-cox method, incorporating survival time, survival status, and gene expression data. Furthermore, we implemented a 10-fold cross-validation to determine the optimal model. In addition, we constructed a nomogram to predict 1-, 3-, and 5-year survival rates of GC patients based on TNM classification, age, gender, risk characteristics, and so on.

Analysis of immune cell infiltration

We used the CIBERSORT algorithm to assess the proportions of 22 immune cells. Additionally, we employed the ESTIMATE algorithm to calculate the differences in estimated scores, immune scores, and stromal scores. Furthermore, the Spearman correlation test was used to determine the correlations between risk scores and immune cell levels.

Analysis of drug sensitivity

The half-maximal inhibitory concentration (IC50) values were evaluated to reflect the response to chemotherapy and immunotherapy drugs. We used the R package "pRRophetic" to predict the IC50 of different drugs in GC samples to evaluate the relationship between m6A/m5C/m1A/m7G-related genes and drug sensitivity.

Validation of m6A/m5C/m1A/m7G-related prognostic genes with immunohistochemical staining

Immunohistochemical staining data of GC and normal tissues were obtained from HPA (http://www.proteinatlas.org/). We validated m6A/m5C/m1A/m7G-related prognostic genes at the protein expression level. There were four degrees of staining: high, intermediate, low, and not detected.

Statistical analysis

Kaplan- Meier curves were used to analyze the overall survival

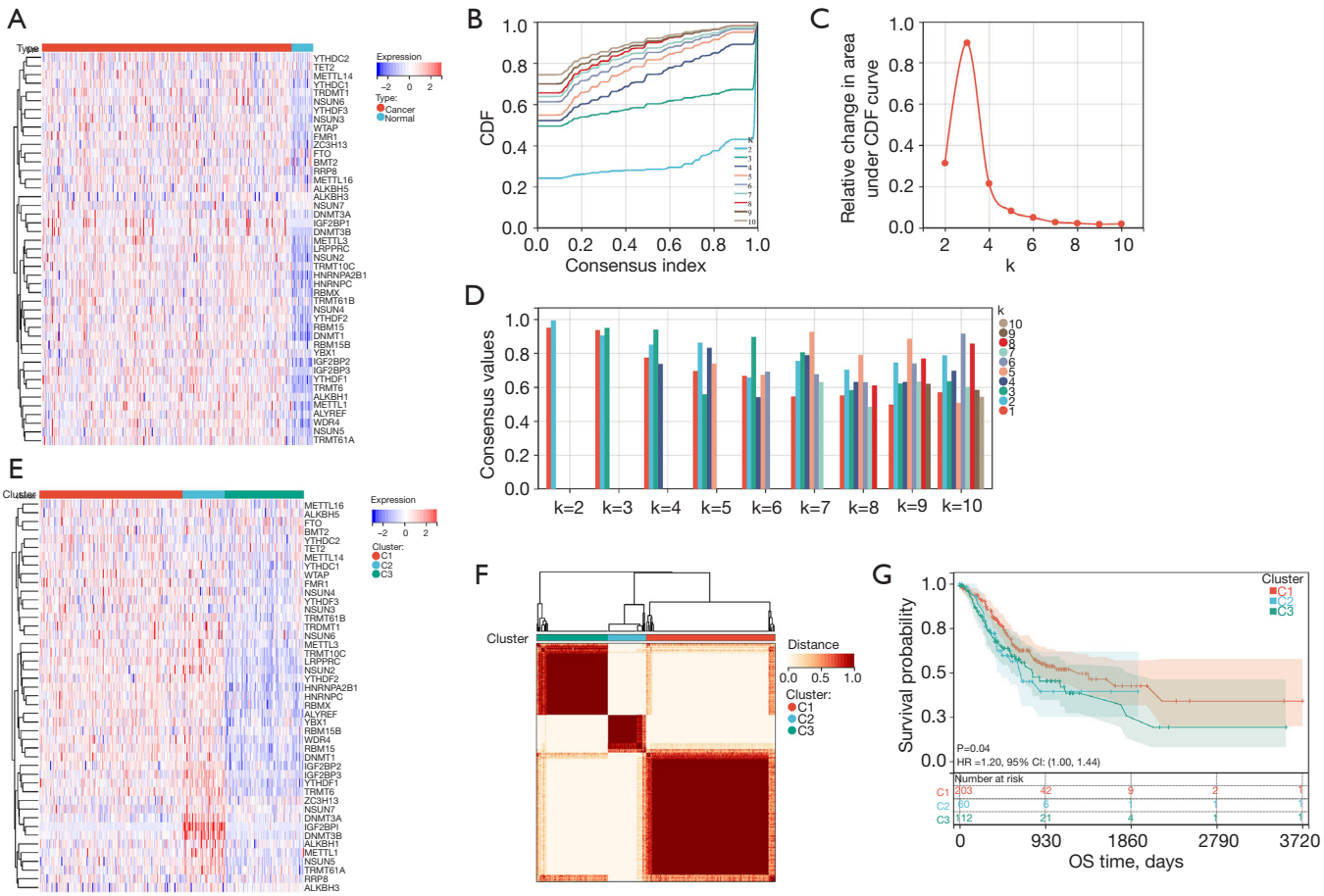

Figure 1 Identification of m6A/m5C/m1A/m7G-related subtypes by consensus clustering. (A) Heatmap of the expression of 45 m6A/m5C/m1A/m7G-related genes in GC samples, including tumor and normal samples; (B,C) cluster analysis of the CDF indicating the area under the curve and the decreasing trend of Delta at k=2–10 and the decreasing trend of area under the curve and Delta; (D) example cluster consistency plot showing that the consensus value is optimal when k=3; (E) heatmap of the expression of 45 m6A/m5C/m1A/m7G-related genes in the three isoforms; (F) consensus matrix for optimal k=3; (G) Kaplan-Meier curves of overall survival for the three subtypes (P=0.04). GC, gastric cancer; CDF, cumulative distribution function; HR, hazard ratio.

of the GC patients in different groups. Limma were perform differential analysis and identify the DEGs between the different groups. LASSO were used to identify m6A/m5C/m1A/m7G-related prognostic genes of GC patients The relationship between risk score and immune cell infiltration was determined using correlation analysis (P<0.05).

Results

Cluster analysis identified m6A/m5C/m1A/m7G-related subtypes

We analyzed the expression patterns of m6A/m5C/m1A/m7G genes in normal and GC samples. It can be seen that most of the m6A/m5C/m1A/m7G genes were highly expressed in GC compared to normal tissues (*Figure 1A*).

Next, we performed a consensus clustering analysis based on the m6A/m5C/m1A/m7G gene expression and survival data of 375 GC samples. The results showed that the consensus matrix was optimal when K=3 (*Figure 1B-1D*). In addition, the three subtypes exhibited different disulfidptosis gene expression (*Figure 1E*). *Figure 1F* shows the heatmap of the consensus matrix when K=3. We further explored whether the different subtypes of C1, C2, and C3 affected the survival of GC patients. The results of the Kaplan-Meier survival curve analysis are shown in *Figure 1G*, in which C1 showed a better clinical

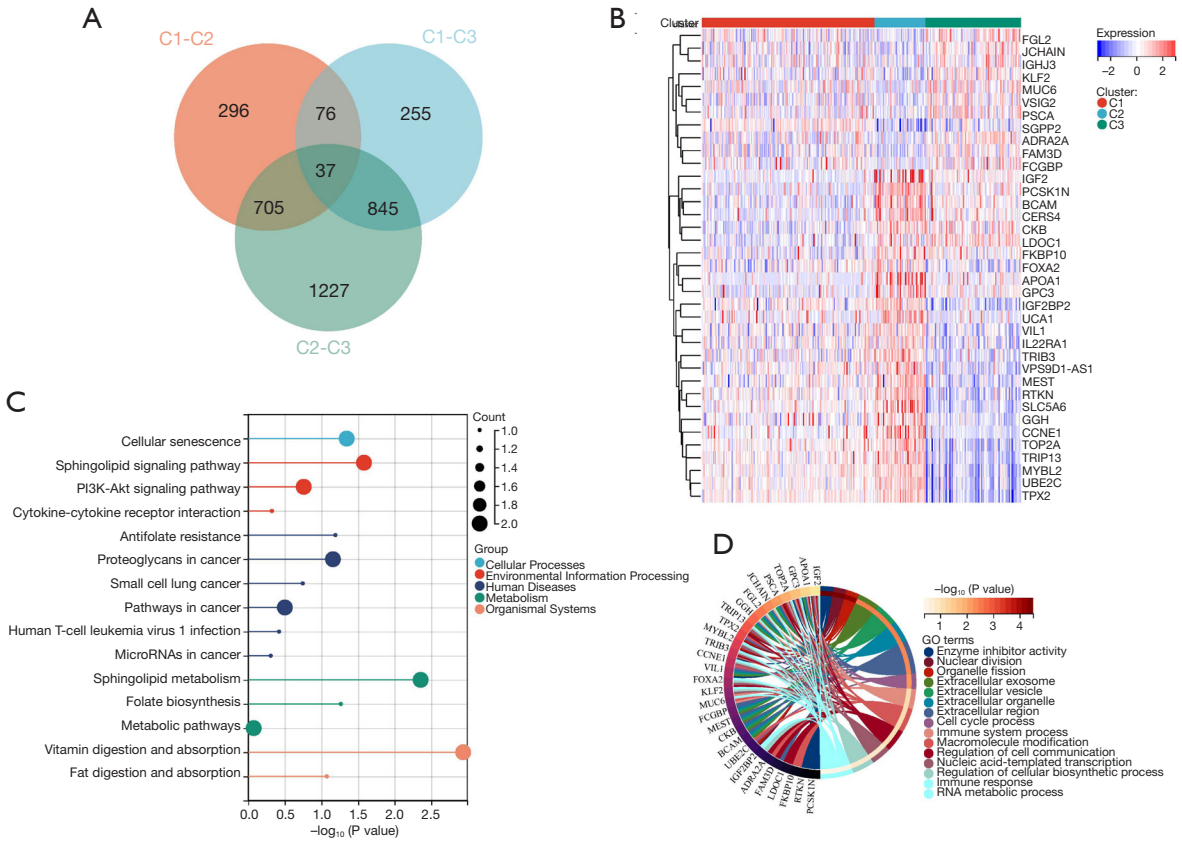

Figure 2 Identification of DEGs and biological pathways between the three m6A/m5C/m1A/m7G subtypes. (A) Venn diagram showing overlapping m6A/m5C/m1A/m7G-related DEGs; (B) heatmap showing the expression of 37 overlapping DEGs between the three isoforms; (C,D) lollipop and circle plots showing the enrichment of KEGG and GO potential signaling pathways. DEGs, differentially expressed genes; KEGG, Kyoto Encyclopedia of Genes and Genomes; GO, Gene Ontology.

outcome (P=0.04).

Differential gene expression and enrichment analysis of m6A/m5C/m1A/m7G-related subtypes

To explore the molecular mechanisms underlying the prognostic differences among the 3 m6A/m5C/m1A/m7G subtypes, we analyzed the DEGs of the three groups and screened a total of 37 DEGs with common intersections (*Figure 2A*). The expression of these 37 genes was also significantly different in each subtype (*Figure 2B*). Further GO and KEGG enrichment analyses indicated that DEGs were involved in extracellular messaging, as well as cancer, immune-related processes such as extracellular exosome, extracellular vesicle, extracellular organelle, immune system process macromolecule modification, cytokine-cytokine receptor interaction, proteoglycans in cancer, human T-cell leukemia virus 1 infection and microRNAs in cancer, among others (*Figure 2C,2D*).

Comparison of somatic mutations, the tumor microenvironment and immune checkpoint among m6A/m5C/m1A/m7G-related subtypes

We analyzed somatic mutations in patients in each group and plotted a waterfall plot of the top 15 genes with the highest mutation frequency (*Figure 3A-3C*). In group C1, *TTN*, *TP53*, *MUC16*, *ARID1A* and *LRP1B* were the most frequently mutated genes. And in group C2, *TP53* was the gene with the highest mutation frequency of 77.6%, which far exceeded the *TP53* mutation frequency in other groups (47.9%, 36.8%). In addition, *SYNE1* and *CSMD3* were the genes with the 5th highest mutation frequency in the C2 and C3 groups, respectively.

We went on to explore the tumor microenvironment in both subtypes. First, the C2 group had lower immune

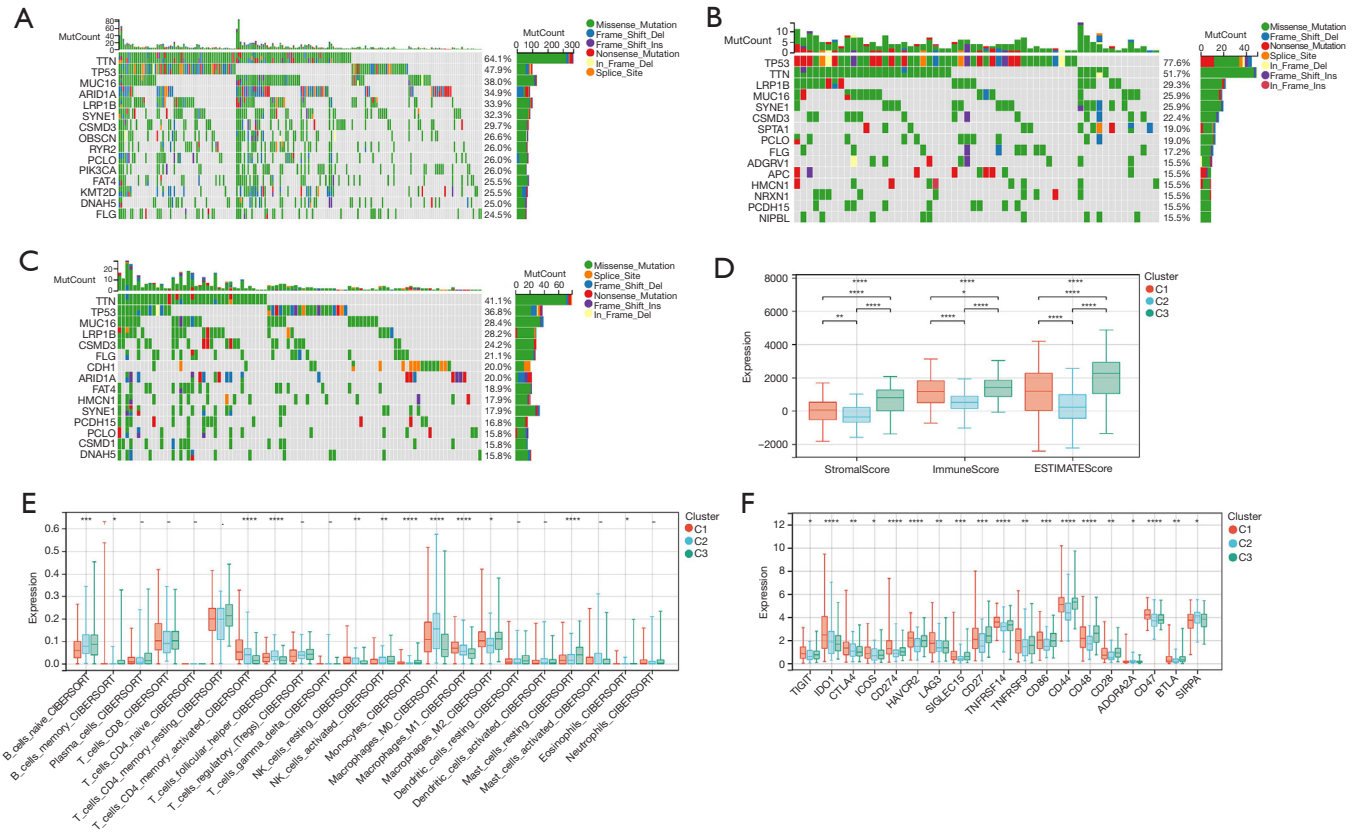

Figure 3 Somatic mutations and immune infiltration of the three m6A/m5C/m1A/m7G subtypes. (A-C) Mutation map waterfall plot showing the 15 most common mutated genes in GC differing between groups C1, C2, and C3; (D) ESTIMATE box-and-line plot showing the IMMUNE SCORE, STOMAL SCORE, and ESTIMATE SCORE of the infiltrating different subtypes; (E) CIBERSORT box plot showing the differences in the infiltration of 22 immune cells among the three subtypes; (F) box plot showing the differences in the expression of some immune checkpoints in the three subtypes. *, P<0.05; **, P<0.01; ***, P<0.001; ****, P<0.0001; "-", not significant. GC, gastric cancer.

scores, stromal scores, and estimated scores than the other groups, while the C3 group had the highest of all. Surprisingly, the C1 group, which had the best survival, was in between the two groups (*Figure 3D*). We next visualized the differences in immune cell infiltration between the two groups using the CIBERSORT method with a box-and-line plot (*Figure 3E*), showing that CD8+ T cells, activated CD4+ memory T cells, resting NK cells, M1 macrophages, and M2 macrophages in group C1 infiltration was higher than in the other groups, while naive B cells and resting mast cells showed the opposite trend.

Finally, we evaluated the relationship of immune checkpoints between each subgroup. As shown in *Figure 3F*, the vast majority of immune checkpoints were most highly expressed in the C1 group. Immunotherapy may be more effective for patients in the C1 group.

Construction and validation of the m6A/m5C/m1A/m7G-related risk signature (MRRS)

In this study, survival time, survival status and gene expression data were integrated and regression analysis was performed using the LASSO-cox method (*Figure 4A*,*4B*). We set the Lambda value to 0.043759414226974, and finally obtained four m6A/m5C/m1A/m7G-related prognostic genes: *SLC5A6*, *FKBP10*, *GPC3*, and *GGH*. The model equation is as follows: Risk Score = −0.0714901538218786×*SLC5A6*+0.0673930236411382×*FKBP10*+0.0651047201271496×*GPC3*-0.0162831756810742×*GGH*.

Next, we examined the relationship between survival status and risk score. It could be observed that with the increase of risk score, the survival of patients decreased significantly. We found that *FKBP10* and *GPC3* were risk

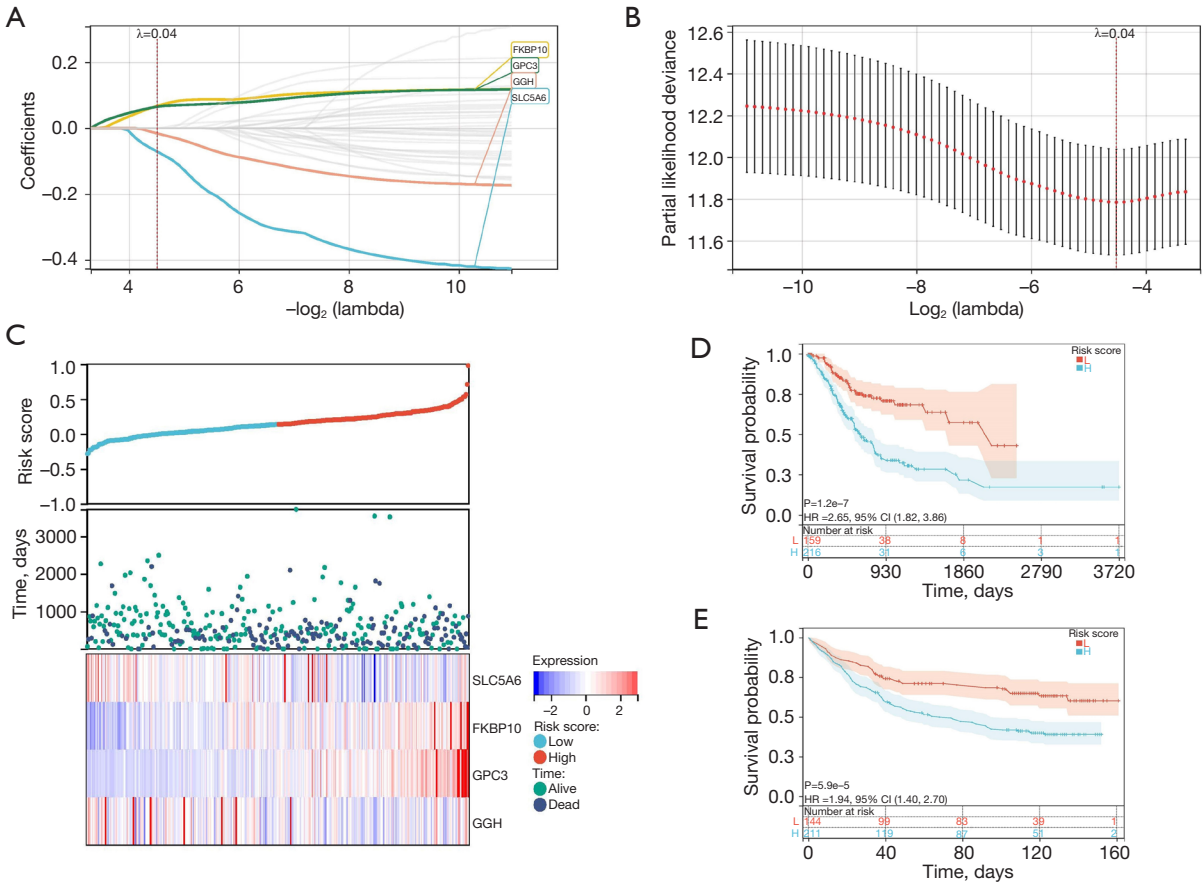

Figure 4 Construction and validation of the MRRS. (A,B) LASSO-Cox analysis of four m6A/m5C/m1A/m7G-related prognostic genes extracted; (C) prognostic heatmap showing the relationship between different risk scores, patient survival, and gene expression changes in the m6A/m5C/m1A/m7G-related risk model; (D,E) Kaplan-Meier curves for MRRS in the training dataset TCGA-STAD and validation dataset GSE84433. MRRS, m6A/m5C/m1A/m7G-related risk signature; LASSO, least absolute shrinkage and selection operator; TCGA-STAD, The Cancer Genome Atlas-Stomach Adenocarcinoma; HR, hazard ratio.

factors with a trend of up-regulation of expression with increasing risk score. On the contrary, *SLC5A6* and *GGH* were protective factors and showed a down-regulation trend in expression with increasing risk score (*Figure 4C*). In addition, we further determined the prognostic significance of MRRS for GC patients using Kaplan-Meier analysis. In TCGA-STAD, the low-risk cohort predicted better survival prognosis ($P=1.2\times10^{-7}$) (*Figure 4D*), and the survival results in the GSE84433 validation set showed the same trend ($P=5.9\times10^{-5}$) (*Figure 4E*). It indicates that our developed MRRS has good recognition performance.

The association of MRRS with prognosis

We performed a multifactorial Cox analysis, and the results showed that the m6A/m5C/m1A/m7G-associated risk score was an independent prognostic predictor of OS in GC patients (*Figure 5A*). In addition, we established a nomogram based on TNM classification, age, gender, and risk characteristics (*Figure 5B*). And calibration curves (*Figure 5C*) and ROC analysis (*Figure 5D*) were performed. The calibration curves showed good agreement between the predicted and actual GC survival cohorts. In the ROC analysis, the AUC values for 1, 3, and 5 years were 0.69,

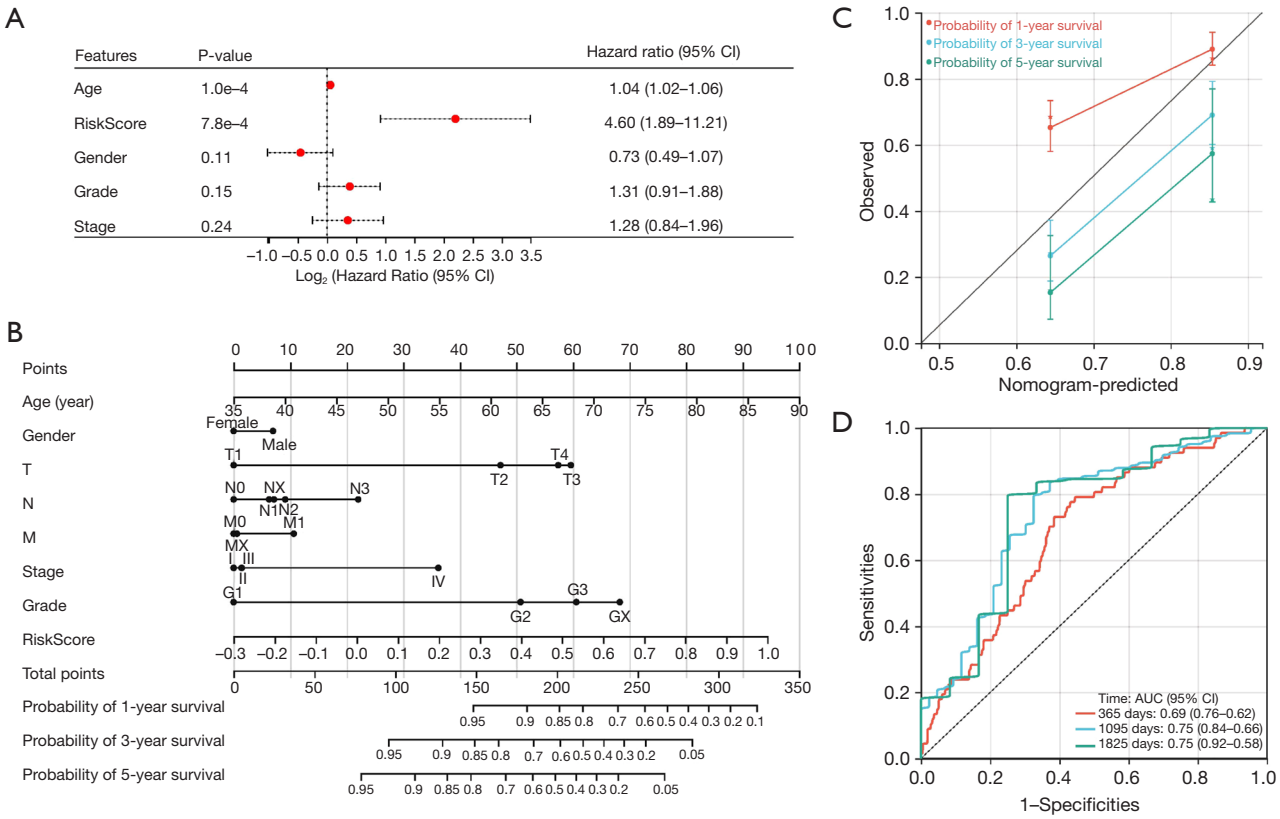

Figure 5 Association of MRRS with GC prognosis. (A) Multivariate Cox analysis to assess the independent prognostic value of MRRS in patients with GC; (B-D) nomo plots, calibration plots, and time-dependent ROC curve analyses used to predict 1-, 3-, and 5-year survival probabilities of patients. MRRS, m6A/m5C/m1A/m7G-related risk signature; GC, gastric cancer; ROC, receiver operating characteristic.

0.75, and 0.75, respectively. Thus, these results suggest that MRRS has good performance in predicting the survival rate of GC patients.

The correlation of MRRS with tumor microenvironment and drug sensitivity

Given the role of m6A/m5C/m1A/m7G-related genes in the immune microenvironment, we further analyzed the correlation between MRRS and immune cell infiltration. The results showed that the risk score was positively correlated with the number of activated CD4+ memory T cells, T follicular helper cells, and resting NK cells, and negatively correlated with resting mast cells (*Figure 6A-6D*). This was further confirmed in the GSE84433 validation set (*Figure 6E-6H*). Interestingly, this is very similar to the immune cell infiltration in group C1 above.

Next, we screened 16 compounds based on the difference in predictive values of IC50 in the high- and low-risk groups. Drug sensitivity analysis showed (*Figure 7*) that patients in the low-risk group were susceptible to Src family selective Lck inhibitor (A-770041), AKT inhibitor VIII, Raf kinase inhibitor (AZ628), saracatinib (AZD-0530), PPM1D inhibitor (CCT007093), dasatinib, elesclomol, Wnt/β-catenin inhibitor (FH-535), and Bcr-Abl inhibitor (GNF-2) were more sensitive than the high-risk group. Conversely, patients in the high-risk group were more sensitive to Bcl-2 protein family inhibitor (ABT-263), Afatinib (BIBW 2992), HSP90ATPase activity inhibitor (CCT018159), doxorubicin, etoposide, lenalidomide, methotrexate (MTX) was higher than that of the low-risk group. This may help to guide individualized medication for both groups.

Validation of m6A/m5C/m1A/m7G-related prognostic genes at the protein levels

To validate the possible relevant biological functions

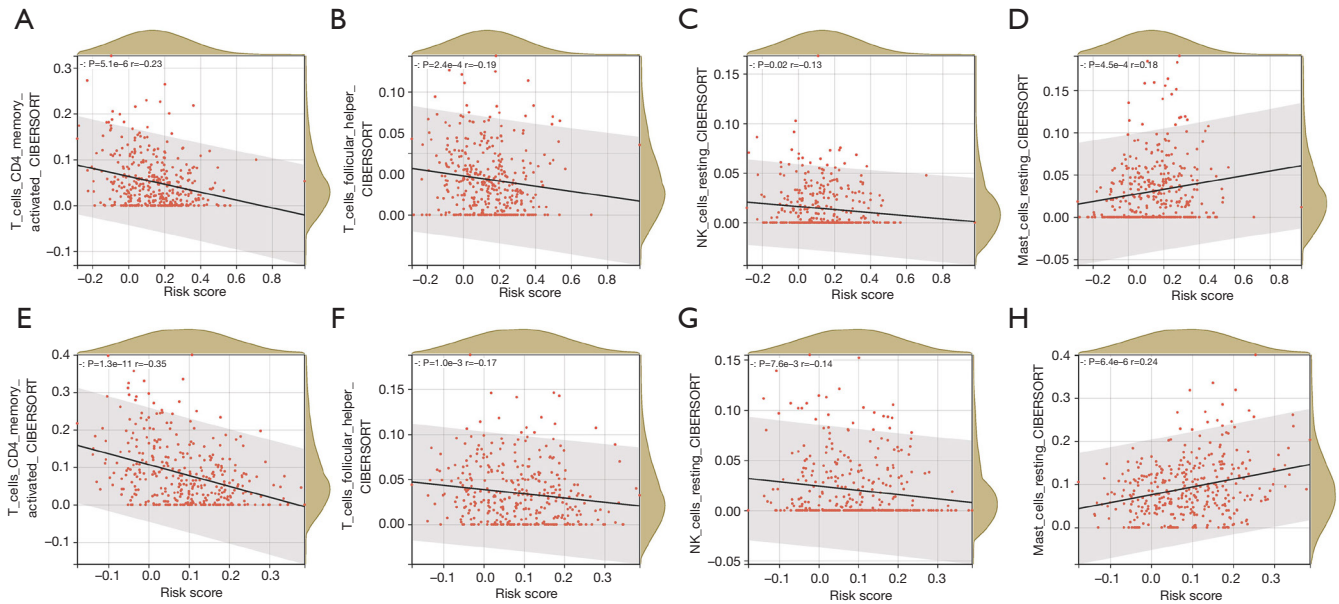

Figure 6 Association of MRRS with tumor microenvironment. Scatterplot showing the correlation of risk score with the infiltration of activated CD4$^+$ memory T cells, follicular helper T cells, resting NK cells and resting mast cells, (A-D) and further validated by the GSE84433 cohort (E-H). MRRS, m6A/m5C/m1A/m7G-related risk signature; NK, natural killer.

of prognostic genes in our MRRS, we evaluated the protein expression levels of m6A/m5C/m1A/m7G-related prognostic genes in normal tissues and GC using HPA immunohistochemical staining data (*Figure 8*). The results showed that *FKBP10* was significantly elevated in GC tissues and *GGH* expression was decreased in GC tissues, which was consistent with our analysis above. In addition, *SLC5A6* did not differ in tumor tissues and normal tissues. Unfortunately, we did not obtain *GPC3* immunohistochemical staining data. We reasonably infer that *FKBP10* and *GGH* may play an important role in GC. The above results demonstrate that the MRRS we developed has a more accurate predictive function for potential prognostic and therapeutic markers of GC.

Discussion

GC, one of the most important cancers of the digestive system, is still a major global health problem. Researchers have been working tirelessly to find biological targets that can predict or improve the prognosis of GC patients. Encouragingly, various correlation models on cancer prognosis have been developed (33-36), which are of great help in developing potential therapeutic targets for GC.

Post-transcriptional modifications of RNA are an important part of the field of epigenetics. Among them, methylation modifications are the most common, and m6A is the most prevalent form of methylation modification and the most intensively studied type of methylation modification. While m6A/m5C/m1A/m7G combines four different methylation modifications, which has been less studied at present, the emergence of this combined methylation mechanism provides new ideas for cancer treatment. Moreover, its specific involvement in GC, the mechanism of occurrence and the pathways involved are still unknown.

Methylation plays a crucial regulatory role in various cellular processes and in the progression of human diseases, and it plays a potentially pivotal role in disease by regulating the expression of proto-oncogenes and tumour-suppressor genes through methyltransferases and demethyltransferases. The aim of tumour immunotherapy is to control and eliminate tumours by restarting and maintaining the tumour immune cycle and restoring normal anti-tumour immune responses. Methylated RNA modifications have implications for immunotherapy (18,27). Therefore, we focused on the potential role of methylation modification genes associated with prognosis and immune infiltration in GC patients.

In this study, we identified three m6A/m5C/m1A/m7G subgroups by consistent clustering based on the expression

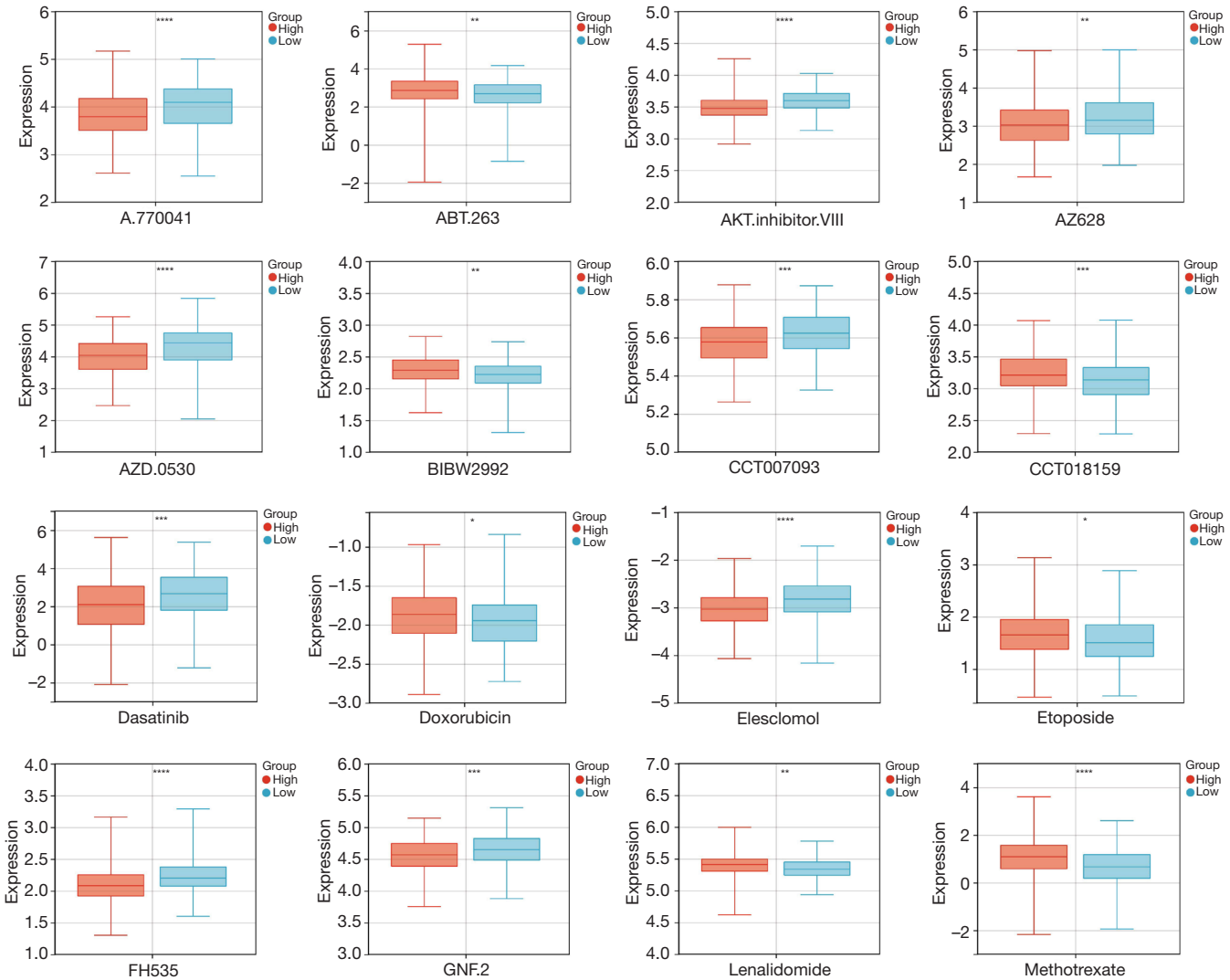

Figure 7 Box line plot showing the results of drug sensitivity analysis for GC patients in the high-risk score group and low-risk score group. *, P<0.05; **, P<0.01; ***, P<0.001; ****, P<0.0001. GC, gastric cancer.

of 45 m6A/m5C/m1A/m7G-related genes, which were significantly differentially expressed at different levels compared with normal tissues (*Figure 1A*). We were then surprised to find that patients with different subtypes of GC had different survival, immune cell infiltration outcomes, and prognosis (*Figure 1G*, *Figure 3*). Next, we identified the DEGs in the three groups using the limma method and finalized four genes, *SLC5A6*, *FKBP10*, *GPC3*, and *GGH*, using the Cox-LASSO method, and constructed MRRS based on them. Some of these genes have been suggested to play a role in cancer or inflammation by influencing the immune response. For example, *FKBP10* has a key role in translational reprogramming and lung cancer growth (38). In addition, *FKBP10* interacts with Hsp47 and activates the AKT-CREB-PCNA signaling pathway, which is involved in the proliferation of glioma cells (39). Elevated expression of *GPC3* has been associated with a poor prognosis of hepatocellular carcinoma (HCC) (40). Overexpression of *GGH* is a risk factor for extranodal extension of oral squamous cell carcinoma (41). On the other hand, *GGH* is important for the chemosensitivity of acute lymphoblastic leukemia (ALL) cells, and lack of *GGH* causes significant resistance to MTX and rituximab (RTX) in ALL cells (42).

Taken together, the results of these 4 genes showed

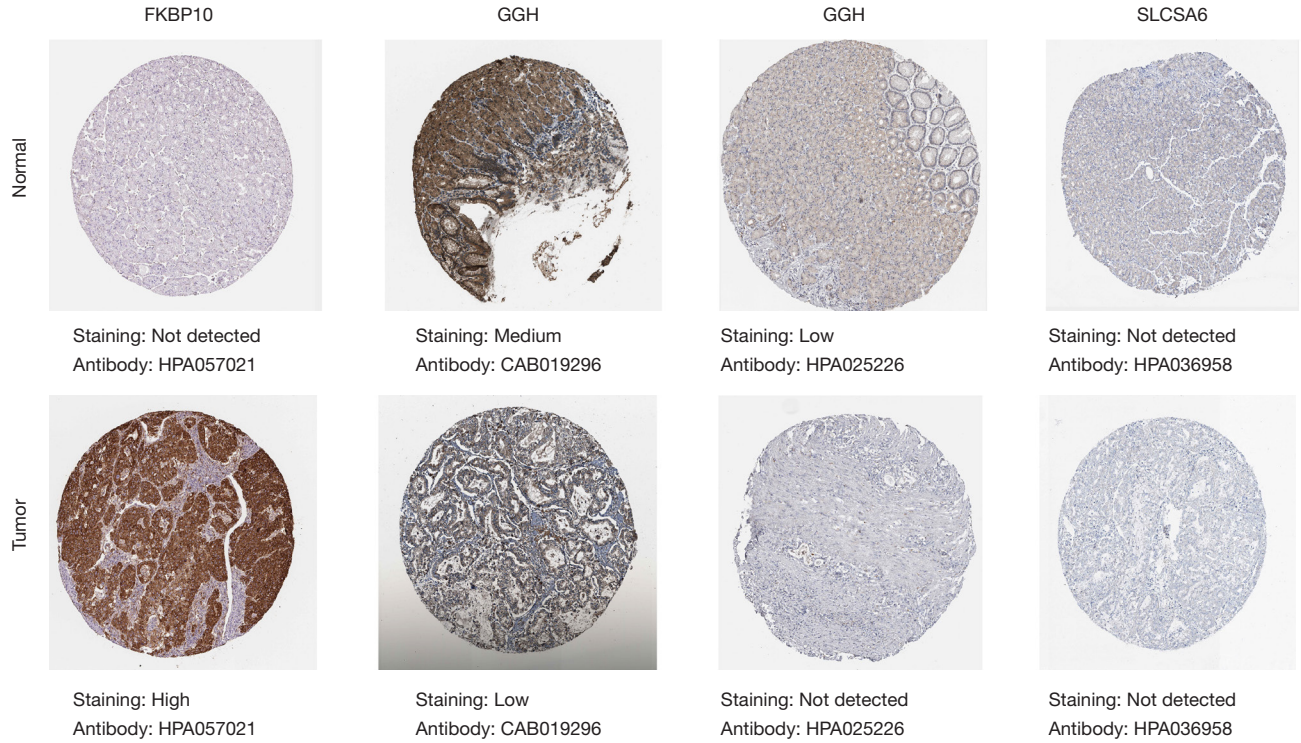

Figure 8 Validation of m6A/m5C/m1A/m7G-associated prognostic genes at the protein expression level. Representative immunohistochemistry images of and gastric cancer (GC) tissues sourced from the Human Protein Atlas database (https://www.proteinatlas.org/). Image credit goes to the Human Protein Atlas. The links to the individual normal and tumor tissues of each protein are provided for *FKBP10* (https://www.proteinatlas.org/ENSG00000141756-FKBP10/tissue/stomach; https://www.proteinatlas.org/ENSG00000141756-FKBP10/pathology/stomach+cancer), *GGH* (https://www.proteinatlas.org/ENSG00000137563-GGH/tissue/stomach; https://www.proteinatlas.org/ENSG00000137563-GGH/pathology/stomach+cancer#ihc), and *SLC5A6* (https://www.proteinatlas.org/ENSG00000138074-SLC5A6/tissue/stomach; https://www.proteinatlas.org/ENSG00000138074-SLC5A6/pathology/stomach+cancer), respectively. Scale bar, 200 μm. Staining degree: high, medium, low, and not detected.

that our MRRS had a better survival prognosis in the low-risk cohort (*Figure 4D*), which we further confirmed in the validation set (*Figure 4E*). The results of this study suggest that m6A/m5C/m1A/m7G can be used as biomarkers for the diagnosis and prognosis of GC and reveal a feasible therapeutic option that may be related to the modulation of the tumor microenvironment.

GO, KEGG analysis showed that DEGs in the three subgroups were significantly enriched in terms of their involvement in extracellular messaging, as well as cancer and immune-related processes. such as extracellular exosome, extracellular vesicle, extracellular organelle, immune system process macromolecule modification, cytokine-cytokine receptor interaction, proteoglycans in cancer, human T-cell leukemia virus 1 infection, and microRNAs in cancer, to name a few (*Figure 2C,2D*). This may explain to some extent the better survival of GC patients in group C1.

Our CIBERSORT box plot (*Figure 3E*) showed that CD8+ T cells, activated CD4+ memory T cells, resting NK cells, M1 macrophages, and M2 macrophages were infiltrated to a higher extent in the C1 group than in the other groups, whereas naive B cells and resting mast cells showed the opposite trend. CD8+ T cells can produce toxic molecules, such as perforin, that cause apoptosis in target cells (43,44). Natural killer cells are highly efficient cell populations used in cancer immunotherapy; memory CD4+ T cells produce a memory response to the immune response and contribute to protective immunity by responding faster and to a greater extent than the initial response (45,46). The main function of M1 macrophages is to kill bacteria and pathogens and produce oxygen free radicals and a range of inflammatory cytokines, whereas M2 macrophages are

mainly involved in anti-inflammatory and repair processes, promoting tissue repair and regeneration (47-49). This may also explain the better survival of GC patients in the C1 group as well. This is because more immune cells were infiltrated in the C1 group. More importantly, the relationship between the various subgroups and the immune checkpoints (*Figure 3F*) showed that the vast majority of the immune checkpoints were most highly expressed in the C1 group. Immunotherapy may work better for patients in the C1 group, consistent with the conclusions above.

Given the role of m6A/m5C/m1A/m7G-related isoforms in the immune microenvironment, we further analyzed the correlation between MRRS and immune cell infiltration. The results showed that the risk score was positively correlated with the number of activated CD4+ memory T cells, T follicular helper cells, and resting NK cells, and negatively correlated with resting mast cells (*Figure 6A-6D*). This was further confirmed in the GSE84433 validation set (*Figure 6E-6H*). The immune cell infiltration in the C1 group is similar to what was observed here. We screened 16 compounds based on the difference in predicted IC50 values between the high and low risk groups. The high risk group was more sensitive to 7 compounds, while the low risk group was more sensitive to 9 compounds. *Figure* 7 illustrates how this information can guide personalized medication for both groups. Finally, we evaluated the protein expression levels of prognostic genes related to m6A, m5C, m1A, and m7G in normal tissues and GC using HPA immunohistochemical staining data. The results suggest that *FKBP10* and *GGH* may play important roles in GC. These results demonstrate that the MRRS we developed has a more accurate predictive function for potential prognostic and therapeutic markers of GC.

However, it is important to acknowledge the limitations of this study. Bioinformatics analysis is a widely used tool for high-precision data analysis and prediction, and can even aid in the exploration of potential biomarkers. Nevertheless, it is recommended that future studies employ real-time polymerase chain reaction (PCR), western blot, and other experimental methods to verify the findings in cell and animal experiments. Secondly, our methylation-related model lacks external validation. In addition, we need to study the related molecular mechanisms to determine how the markers we identified are involved in GC. In future studies, we will further explore their mechanisms of action in GC.

Conclusions

In conclusion, our study has highlighted the association between m6A/m5C/m1A/m7G-related subtypes and changes in the GC immunotumor microenvironment. We have also constructed the MRRS and validated its effectiveness in different cohorts. This tool is valuable in predicting survival, immune infiltration, drug sensitivity, and other factors in GC patients. These results may help to deepen our understanding of m6A/m5C/m1A/m7G methylation and provide new strategies for personalized therapy.

Acknowledgments

Funding: None.

Footnote

Reporting Checklist: The authors have completed the TRIPOD reporting checklist. Available at https://tcr.amegroups.com/article/view/10.21037/tcr-23-2325/rc

Peer Review File: Available at https://tcr.amegroups.com/article/view/10.21037/tcr-23-2325/prf

Conflicts of Interest: Both authors have completed the ICMJE uniform disclosure form (available at https://tcr.amegroups.com/article/view/10.21037/tcr-23-2325/coif). The authors have no conflicts of interest to declare.

Ethical Statement: The authors are accountable for all aspects of the work in ensuring that questions related to the accuracy or integrity of any part of the work are appropriately investigated and resolved. The study was conducted in accordance with the Declaration of Helsinki (as revised in 2013).

References

1. Siegel RL, Miller KD, Fuchs HE, et al. Cancer statistics, 2022. CA Cancer J Clin 2022;72:7-33.
2. Yang WJ, Zhao HP, Yu Y, et al. Updates on global epidemiology, risk and prognostic factors of gastric cancer. World J Gastroenterol 2023;29:2452-68.
3. Shin WS, Xie F, Chen B, et al. Updated Epidemiology of Gastric Cancer in Asia: Decreased Incidence but Still a Big Challenge. Cancers (Basel) 2023;15:2639.
4. Ilson DH. Advances in the treatment of gastric cancer: 2022-2023. Curr Opin Gastroenterol 2023;39:517-21.
5. Guan WL, He Y, Xu RH. Gastric cancer treatment: recent progress and future perspectives. J Hematol Oncol 2023;16:57.
6. Joshi SS, Badgwell BD. Current treatment and recent progress in gastric cancer. CA Cancer J Clin 2021;71:264-79.
7. Siebenhüner AR, De Dosso S, Helbling D, et al. Advanced Gastric Cancer: Current Treatment Landscape and a Future Outlook for Sequential and Personalized Guide: Swiss Expert Statement Article. Oncol Res Treat 2021;44:485-494. Correction appears in Oncol Res Treat 2022;45:62.
8. Tan Z. Recent Advances in the Surgical Treatment of Advanced Gastric Cancer: A Review. Med Sci Monit 2019;25:3537-41.
9. Song Z, Wu Y, Yang J, et al. Progress in the treatment of advanced gastric cancer. Tumour Biol 2017;39:1010428317714626.
10. Lei ZN, Teng QX, Tian Q, et al. Signaling pathways and therapeutic interventions in gastric cancer. Signal Transduct Target Ther 2022;7:358.
11. Yuan L, Xu ZY, Ruan SM, et al. Long non-coding RNAs towards precision medicine in gastric cancer: early diagnosis, treatment, and drug resistance. Mol Cancer 2020;19:96.
12. Zeng Y, Jin RU. Molecular pathogenesis, targeted therapies, and future perspectives for gastric cancer. Semin Cancer Biol 2022;86:566-82.
13. Röcken C. Predictive biomarkers in gastric cancer. J Cancer Res Clin Oncol 2023;149:467-81.
14. Barbieri I, Kouzarides T. Role of RNA modifications in cancer. Nat Rev Cancer 2020;20:303-22.
15. Zhao BS, Roundtree IA, He C. Post-transcriptional gene regulation by mRNA modifications. Nat Rev Mol Cell Biol 2017;18:31-42. Correction appears in Nat Rev Mol Cell Biol 2018;19:808.
16. Chen Y, Jiang Z, Yang Y, et al. The functions and mechanisms of post-translational modification in protein regulators of RNA methylation: Current status and future perspectives. Int J Biol Macromol 2023;253:126773.
17. Boulias K, Greer EL. Biological roles of adenine methylation in RNA. Nat Rev Genet 2023;24:143-60.
18. Yang B, Wang JQ, Tan Y, et al. RNA methylation and cancer treatment. Pharmacol Res 2021;174:105937.
19. Zhou W, Wang X, Chang J, et al. The molecular structure and biological functions of RNA methylation, with special emphasis on the roles of RNA methylation in autoimmune diseases. Crit Rev Clin Lab Sci 2022;59:203-18.
20. An Y, Duan H. The role of m6A RNA methylation in cancer metabolism. Mol Cancer 2022;21:14.
21. Ma S, Chen C, Ji X, et al. The interplay between m6A RNA methylation and noncoding RNA in cancer. J Hematol Oncol 2019;12:121.
22. Zhang Q, Liu F, Chen W, et al. The role of RNA m(5) C modification in cancer metastasis. Int J Biol Sci 2021;17:3369-80.
23. Cheng W, Gao A, Lin H, et al. Novel roles of METTL1/WDR4 in tumor via m(7)G methylation. Mol Ther Oncolytics 2022;26:27-34.
24. Li J, Zhang H, Wang H. N(1)-methyladenosine modification in cancer biology: Current status and future perspectives. Comput Struct Biotechnol J 2022;20:6578-85.
25. Zaccara S, Ries RJ, Jaffrey SR. Reading, writing and erasing mRNA methylation. Nat Rev Mol Cell Biol 2019;20:608-624.Correction appears in Nat Rev Mol Cell Biol 2023;24:770.
26. Shi H, Wei J, He C. Where, When, and How: Context-Dependent Functions of RNA Methylation Writers, Readers, and Erasers. Mol Cell 2019;74:640-50.
27. Zhuang H, Yu B, Tao D, et al. The role of m6A methylation in therapy resistance in cancer. Mol Cancer 2023;22:91.
28. Petri BJ, Klinge CM. m6A readers, writers, erasers, and the m6A epitranscriptome in breast cancer. J Mol Endocrinol 2022;70:e220110.
29. Chen X, Li A, Sun BF, et al. 5-methylcytosine promotes pathogenesis of bladder cancer through stabilizing mRNAs. Nat Cell Biol 2019;21:978-90.
30. Allegri L, Baldan F, Molteni E, et al. Role of m6A RNA Methylation in Thyroid Cancer Cell Lines. Int J Mol Sci 2022;23:11516.
31. Liang W, Yi H, Mao C, et al. Research Progress of RNA Methylation Modification in Colorectal Cancer. Front

Pharmacol 2022;13:903699.
32. Teng C, Kong F, Mo J, et al. The roles of RNA N(6)-methyladenosine in esophageal cancer. Heliyon 2022;8:e11430.
33. Huang Z, Pan J, Wang H, et al. Prognostic Significance and Tumor Immune Microenvironment Heterogenicity of m5C RNA Methylation Regulators in Triple-Negative Breast Cancer. Front Cell Dev Biol 2021;9:657547.
34. Chong W, Shang L, Liu J, et al. m(6)A regulator-based methylation modification patterns characterized by distinct tumor microenvironment immune profiles in colon cancer. Theranostics 2021;11:2201-17.
35. Wang Z, Zhang M, Seery S, et al. Construction and validation of an m6A RNA methylation regulator prognostic model for early-stage clear cell renal cell carcinoma. Oncol Lett 2022;24:250.
36. Zhou Y, Dai X, Lyu J, et al. Construction and validation of a novel prognostic model for thyroid cancer based on N7-methylguanosine modification-related lncRNAs. Medicine (Baltimore) 2022;101:e31075.
37. Li J, Zuo Z, Lai S, et al. Differential analysis of RNA methylation regulators in gastric cancer based on TCGA data set and construction of a prognostic model. J Gastrointest Oncol 2021;12:1384-97.
38. Ramadori G, Ioris RM, Villanyi Z, et al. FKBP10 Regulates Protein Translation to Sustain Lung Cancer Growth. Cell Rep 2020;30:3851-3863.e6.
39. Cai HQ, Zhang MJ, Cheng ZJ, et al. FKBP10 promotes proliferation of glioma cells via activating AKT-CREB-PCNA axis. J Biomed Sci 2021;28:13.
40. Fu Y, Urban DJ, Nani RR, et al. Glypican-3-Specific Antibody Drug Conjugates Targeting Hepatocellular Carcinoma. Hepatology 2019;70:563-76.
41. Burhanudin NA, Zaini ZM, Rahman ZAA, et al. Overexpression of gamma glutamyl hydrolase predicts extranodal extension in squamous cell carcinoma of the oral cavity. Oral Surg Oral Med Oral Pathol Oral Radiol 2022;134:725-32.
42. Wang S, Chen Y, Fang H, et al. A γ-glutamyl hydrolase lacking the signal peptide confers susceptibility to folates/antifolates in acute lymphoblastic leukemia cells. FEBS Lett 2022;596:437-48.
43. Notarbartolo S, Abrignani S. Human T lymphocytes at tumor sites. Semin Immunopathol 2022;44:883-901.
44. Reina-Campos M, Scharping NE, Goldrath AW. CD8(+) T cell metabolism in infection and cancer. Nat Rev Immunol 2021;21:718-38.
45. Preethy S, Dedeepiya VD, Senthilkumar R, et al. Natural killer cells as a promising tool to tackle cancer-A review of sources, methodologies, and potentials. Int Rev Immunol 2017;36:220-32.
46. Künzli M, Masopust D. CD4(+) T cell memory. Nat Immunol 2023;24:903-14.
47. Xia Y, Rao L, Yao H, et al. Engineering Macrophages for Cancer Immunotherapy and Drug Delivery. Adv Mater 2020;32:e2002054.
48. Liu J, Geng X, Hou J, et al. New insights into M1/M2 macrophages: key modulators in cancer progression. Cancer Cell Int 2021;21:389.
49. Boutilier AJ, Elsawa SF. Macrophage Polarization States in the Tumor Microenvironment. Int J Mol Sci 2021;22:6995.

Cite this article as: Chen R, Jiang L. A novel m6A/m5C/m1A/m7G-related classification and risk signature predicts prognosis and reveals immunotherapy inclination in gastric cancer. Transl Cancer Res 2024;13(7):3285-3298. doi: 10.21037/tcr-23-2325

